Transportation Geotechnics 41 (2023) 101033

Contents lists available at ScienceDirect

Transportation Geotechnics

journal homepage: www.elsevier.com/locate/trgeo

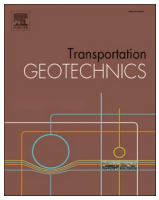

Jointed rock masses as metamaterials – Implications for railway tunnel vibrations

Harry Holmes [a,*], Chrysothemis Paraskevopoulou [a], Mark Hildyard [a], Krishna Neaupane [b], David P. Connolly [a]

[a] University of Leeds, Leeds LS2 9JT, United Kingdom
[b] AECOM, 20 Colmore Circus Queensway, Birmingham B4 6AT, United Kingdom

ARTICLE INFO

Keywords:
Tunnel vibrations
Underground railway
Metamaterials
Ground-borne vibrations
Rock masses

ABSTRACT

Vibrations from underground railways are known to affect receptors located close to the tunnel. Understanding the transmission pathway between these tunnels and receptors is important in determining the magnitude of vibrations which can be transmitted. Rail tunnels can be excavated in a range of geological conditions, including jointed rock masses. Jointed rock masses have been found to display certain resonant characteristics, namely spring resonance. Therefore, this paper studies the resonant characteristics of jointed rock masses using a series of models solved using the combined discrete element-finite difference method and the finite difference method. Modelling assumptions are tested as well as different equivalent material models. It is found that spring resonances occur at the same frequencies as predicted by analytical functions when different modelling assumptions are used. This indicates that the spring resonance effect will prevail in complex rock masses under a range of geological settings. The spring resonance mechanism is found to cause jointed rock masses to behave like periodic metamaterials in respect to the transmission of stress waves, which can operate as a band-pass or low pass filter, depending on the number of joints within the material. New evidence is presented showing that periodic metamaterials exhibit spring resonance. Results for metamaterials in laboratory scale frequency sweep tests are shown to feature high transmission zones occurring at the predicted spring resonant frequency for that material. Finally, the effects of the spring resonance mechanism operating within the jointed rock masses are appraised in the context of vibrations from railway tunnels.

Introduction

With jointed rock masses being common throughout a wide range of geological settings, stress waves generated from within a rock mass are likely to encounter joints at some point in the propagation pathway. Jointed propagation pathways have been found to have the potential to affect the amplitude of stress waves as they are transmitted [1–4]. Many different types of vibration sources can excite a rock mass. These will have the amplitude of their waves modified along the transmission path by effects such as changes in material stiffness, joints, and damping, to name a few. Such sources include, but are not limited to, trains in tunnels [5–9], trains on embankments [10], blasting [11] and construction [12] for synthetic sources and earthquakes [13,14] for natural sources. This research is orientated towards train vibrations, which are shown in Fig. 1. All these sources can excite stress waves at a range of different frequencies. Trains can generate a range of frequencies from a range of different sources, generated at the wheel-rail interface, including wheel corrugation and out of roundness, rail head corrugation and sleeper passage, among others (Fig. 1) [10]. Although frequencies exceed 1 kHz can be generated, much of the frequency content is in the range of 0–250 Hz [15]. Trains can generate ground-borne noise (reradiated noise) and ground vibrations (structural vibrations).

Vibrations propagating through the ground can impact upon receptors located close by. There are well known examples of the destruction caused by earthquakes, although the effects of other sources, which typically generate much lower amplitudes, are less obvious. Rail vibrations for instance have been found to interfere with vibration sensitive structures, such as recording studios and scientific laboratories, which can have a detrimental effect on the use of such buildings [16]. The health of people exposed to ground borne vibrations can also be

* Corresponding author.
E-mail addresses: ee15hth@leeds.ac.uk (H. Holmes), C.Paraskevopoulou@leeds.ac.uk (C. Paraskevopoulou), M.Hildyard@leeds.ac.uk (M. Hildyard), krishna.neaupane@aecom.com (K. Neaupane), D.Connolly@leeds.ac.uk (D.P. Connolly).

https://doi.org/10.1016/j.trgeo.2023.101033
Received 11 April 2023; Received in revised form 9 May 2023; Accepted 19 May 2023
Available online 26 May 2023

impacted. Heart rate has been found to accelerate by up to 3 bpm during sleep, affecting the long term cardiovascular function of exposed populations [15]. There has been a large body of research looking into train vibrations from tunnels; however, the majority of this has been conducted in soft ground tunnelling conditions [5,17,18]. There has been limited work examining trains in tunnels embedded hard in rock tunnelling conditions. Avci et al. [9] studied annoyance from train tunnels embedded in rock, although the role of joints was not investigated, with the rock mass treated as a homogenous layer with a high stiffness. Eitzenberger [7] did study the role of joints in the transmission of stress waves from underground sources. It was shown that joints can affect the propagation of stress waves, with joints acting as wave guides. The results were analysed qualitatively, and no specific resonance effects were identified, although their presence was alluded to.

The transmission of stress waves through joints are well studied, with analytical expressions derived for single joints [19] and multiple joints [1,3,4,20,21]. For linear elastic joints, Pyrak-Nolte et al. [19] showed that energy is transmitted and reflected from a single joint, shown by Eqs. (1) and (2). The energy reflected (R_1) and transmitted (T_1) from one joint is dependent upon the joint stiffness (k), block seismic impedance (z) and wave angular frequency (ω). The $k/z\omega$ term, included in Eqs. (1) and (2), is often referred to as the non-dimensional joint stiffness. The analytical expressions for single joints have been found to agree with numerical modelling results by Cai and Zhao [1], among others.

$$T_1 = \frac{2\frac{k}{z\omega}}{2\frac{k}{z\omega} - i} \tag{1}$$

$$R_1 = \frac{i}{2\frac{k}{z\omega} - i} \tag{2}$$

Where i is $\sqrt{-1}$.

Transmissions through multiple joints have been found to be a complex process, with wave reflections and interactions being possible. Pyrak-Nolte et al. [3] presented equation (3) as an indication of the possible transmission through N joints (T_N), although this does not take into account wave superposition, and addresses the problem as the cumulative reduction in transmission due to each individual joint. Schoenberg and Sayers [22] proposed that joint spacing influences the transmission of stress waves through multiple joints, suggesting that when the wavelength is much larger than the joint spacing an equivalent medium can be assumed.

$$|T_N| = |T_1|^N \tag{3}$$

Cai and Zhao [1] presented analytical expressions for the transmission of stress waves through multiple parallel joints in terms of normalised joint spacing (ξ), given as the joint spacing (s) divided by the wavelength (λ) ($\xi = s/\lambda$). This study considered the amplitude of first arrivals of a single period sine wave. It was also found that for normalised joint spacings of less than 0.3 a high transmission zone exhists. This high transmission zone at a low ξ, which is equivalent to a low frequency, is proposed to be caused by wave superposition effects, with many subsequent studies appearing to corroborate this view [23–27]. On the face of it, this conclusion appears to be divergent from the conclusions of Schoenberg and Sayers [22], as the wavelength associated with a low frequency will be large. The high transmission zone is an effect of the jointing and therefore is not consistent with an equivalent medium where joints will not be discretely modelled, despite the large wavelength.

The use of normalised terms, such as ξ, are widely used in research of stress wave transmission through jointed materials. However, these lack relevance to engineering practice, where excitation sources are often introduced in non-normalised terms, such as frequency or wavelength. Therefore, the findings of these previous studies are not directly applicable to practical situations.

Parastatidis [28] investigated the effects of using equivalent materials on the transmission of stress waves through joints, using a finite difference (FD) model. Three different material models were

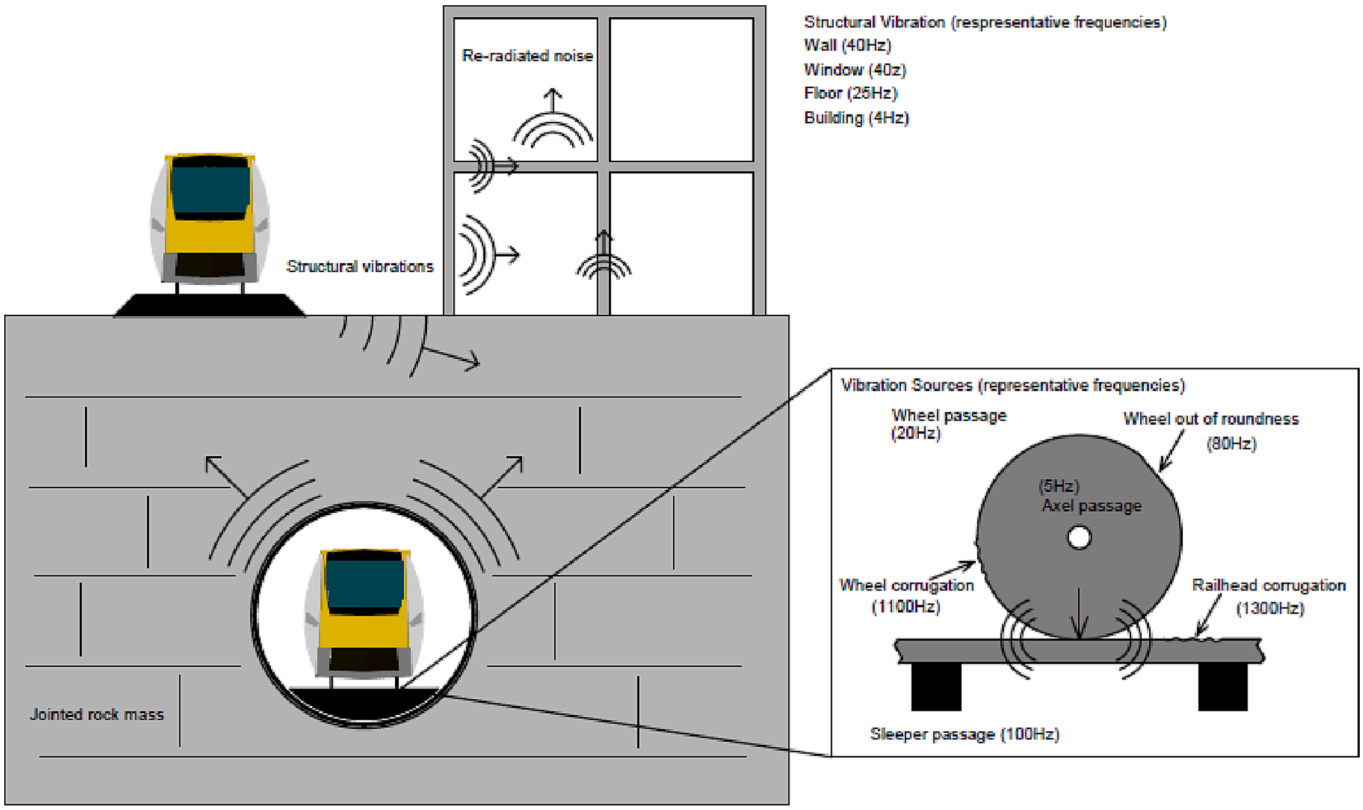

Fig. 1. Source of ground vibrations from trains in jointed rock masses.

investigated: discrete joints, a localised equivalent medium and a homogenous equivalent medium. Discrete joints were modelled using a special element representing joints [29], while the localised and homogenous equivalent mediums were modelled using equivalent transversely isotropic materials. The localised medium applied an equivalent medium to the FD grid nodes which were represented by joints in the discrete joint representation. The homogenous equivalent medium on the other hand applies equivalent material properties to the entire model. In order to capture the effect of the joints the cracks per unit length (1/L) is used, calculated as the surface area of each joint divided by the volume of the equivalent material. The calculation of crack per unit length is shown in Eq. (4), where A and B are the dimensions of the joint surface, C is the length of the equivalent material and N is the number of joints. Finally, the cracks per unit length is used to modify the elastic properties of the medium using the method of Coates and Schoenberg [30].

$$\frac{1}{L} = \frac{ABN}{ABC} \tag{4}$$

Holmes et al. [4] revisited the concept of high transmission of stress waves through jointed rock masses by analysing a wide band excitation source propagating through a 1D model using transfer functions. The use of transfer functions allows the full-transmitted waveform to be analysed, as opposed to only the first arrival as used in previous studies and gives a new way of analysing transmission through joints [1]. This is a useful approach as the full waveform will be incident upon a receiver. A spring resonance mechanism, operating at low frequencies, and an acoustic resonance mechanism, operating at relatively high frequencies, were identified. Analytical expressions for these were presented, shown in Eqs. (5) and (6), for spring resonance, and Eq. (7), for acoustic resonance. The spring resonance mechanism is a newly identified rock mass transmission effect, while the acoustic resonance effect has been identified previously [31–33]. The newly identified spring resonance mechanism raises practical problems for realistic vibration sources, such as trains. Therefore, further analysis is required to determine whether spring resonance arises in more complex scenarios than those previously modelled, which the current study undertakes.

$$K_m X = \alpha M X \tag{5}$$

$$f_n = \frac{1}{2\pi}\sqrt{\alpha_n} \tag{6}$$

$$f_n = \frac{(n - Jn - 1)C_p}{2s} \tag{7}$$

Where K_m = stiffness matrix for joints and blocks; M = mass matrix for joints; X = vector satisfying Eq. (5); f_n = resonant frequency of mode n; α,α_n = eigenvalues and eigenvalue n; n = mode number of resonant frequencies (low frequency + high frequency resonance combined); Jn = number of joints; C_p = p-wave velocity of intact material; s = joint spacing.

Eqs. (5) and (6), for the spring resonance mechanism, give the same number of resonant frequencies as there are blocks within a model. A single block is contained between two joints, so the number of blocks is equal to Jn-1. The blocks between the end joints and the model boundaries behave as part of an infinite rock mass so are effectively not part of the jointed region of the model and not included in this number. Holmes et al. [4] found that when there are a large number of joints the spring resonances merge, giving a high transmission zone at low frequencies.

The body of research presented above shows evidence that jointed rock masses have the potential to modify stress waves as they are transmitted, with Eqs. (5) to (7) providing accurate predictions for the resonances of a jointed material. If it were so desired, an artificial rock mass could be constructed to have a particular set of frequency related properties, which is a similar concept to those used for the design and manufacture of periodic metamaterials [14,34,35]. Jointed rock masses could be considered a natural periodic metamaterial, composed of discrete blocks and joints, capable of transforming stress waves. In acoustics, the parallel jointed rock mass studied by Holmes et al. [4] could be considered a 1D phononic crystal. The jointed rock mass can absorb or transmit different frequencies. With a small number of blocks, this will act as a band-pass filter prohibiting wave frequencies that do not fall within the pass bands, which are coincident with the resonant frequencies of the material. As the number of joints increases the rock mass will transition to an effectively low-pass filter as the resonances begin to overlap one another. Defining jointed rock masses in such a way puts them in the context of current research into metamaterials, a current and fast evolving field of research. Hussein et al. [36] investigated the mass between spring resonance shown by periodic metamaterials, showing these do exist in 1D monatomic lattices. Periodic metamaterials can be used for practical purposes, such as in wave barriers, to shield sensitive structures from the effects of vibrations [14,35,37].

Holmes et al. [4] assumed a one-dimensional (1D) rock mass with infinite joints, and a plane wave. The assumptions adopted are a practical approximation for simplified numerical models studying the effect of joints; however, they are not realistic, as infinite joints and purely plane waves are unlikely in nature. Therefore, there are unanswered questions relating to the applicability of the resonance effects observed in realistic situations, especially considering the original approach adopted when analysing the results, i.e. transfer functions. This study explores the spring resonance mechanism predicted from Eqs. (5) and (6) in further detail by breaking modelling assumptions, such as symmetrical boundaries parallel to wave propagation, infinite joints, and plane waves. In addition to this, equivalent material models, as previously used by Parastatidis [28], are investigated to determine whether they exhibit resonance characteristics. The outcomes are appraised in the context of rail vibrations. With rail vibrations occurring at low frequencies, only the spring resonance mechanism is studied. Acoustic resonance tends to occur at relatively high frequencies, which are likely to be outside the range of frequencies generated by railways. This study explores the likelihood that the spring resonance mechanism occurs in physical systems and therefore will indicate whether it is an effect that needs to be considered in vibrational studies through jointed materials. Considering these highly transmitted frequencies, will allow a more efficient design of mitigation measures for vibration sensitive structures. The effects of the number, stiffness and spacing of joints were investigated by Holme et al [4], so is not studied here.

Methodology

This study uses two different numerical modelling methods to investigate resonance effects. The combined discrete element-finite difference method (DEM-FDM) is used to show how changing the modelling assumptions surrounding boundary conditions and the number of joint sets can affect the response of the model. The finite difference method (FDM) is used to investigate whether models give the same resonances when modelled using equivalent material models. The models in this study are used to investigate the concept of resonance in jointed rock masses and have been previously found to accurately and realistically model stress wave transmission through jointed materials [38,39]. Resonance of a material is a fundamental part of the transmission of a waveform through that material, so considering that the models used in this study can accurately transmit vibrations indicates that, when data is analysed in an appropriate way, resonance effects can be identified.

Detailed descriptions of each of the models used in this study are given below, split into two sections: the first considering discrete joints and testing modelling assumptions, with the second considering equivalent material models. Subtly different model set ups are used for the DEM-FDM and FDM models. This provides an additional check that the resonance effects observed are not modelling artefacts.

Discrete jointed models

Models using two different numerical methods, the FDM, solved using the software WAVE2D [29], and the DEM-FDM, solved using the software UDEC (Universal Discrete Element Code) [40]. Two different numerical codes are used as there are a range of different scenarios being modelled, which the different codes are more suitable for. It has been previously shown that the two methods give comparable results for 1D rock mass transmission problems [4].

The FDM model is excited by a modified Ricker wave, with the DEM-FDM model excited by a Gaussian function, both with a 500 Hz driving frequency. Despite this representing a wider range of frequencies than those generated by rail traffic, this excitation ensures a wide band of frequencies is excited within the model, allowing a wide range of frequencies to be analysed by the transfer functions. These are the same input waves which are used by Holmes et al. [4], with the frequency content of the waves shown in Fig. 2. The two waves do have slightly different frequency content to one another. However, due to the transfer function method used here, the actual frequency content of the waves does not affect the results. As such, the results of the transfer functions can be readily applied to different sources, such as train vibrations. As different numerical models and excitation waveforms are used through this study, any similarity in results cannot be a consequence of the model setups or the excitation. This provides an additional verification to the realism of the resonance mechanisms observed.

Material damping is not applied to any model used, with linear elastic material properties applied to joints and intact blocks, as used by previous studies [1,2,4]. The material properties used in this study are given in Table 1. The use of linear elastic properties is undoubtedly an assumption which requires testing; however, considering a common vibrational source, such as rail vibrations, strains within the rock mass will be low [41]. This will ensure that the response of the material is well approximated by elastic material properties. Even considering a non-linear joint stiffness model, such as the Barton-Bandis model [42], a small portion of the stress–strain relationship for a joint will approximate a linear relationship.

Table 1
Modelling material properties.

Property	Value
Joint Stiffness	1 GPa/m
Joint Spacing	2 m
Number of Joints	2
Intact Material P-Wave Velocity	3328 m/s
Intact Material S-Wave Velocity	1922 m/s
Intact Material Density	2600 kg/m^3

This study attempts to further understand the spring resonance mechanism and determine the robustness of the effect to changing conditions in a rock mass. In order to do this, assumptions adopted by Holmes et al. [4] are examined. The assumptions being tested are symmetrical boundary conditions, infinite joints, and plane waves. To achieve this, three new scenarios are modelled, two solved in the DEM-FDM (Models 2 and 3) and one solved in the FDM (Model 4). The two DEM-FDM models are 1D models, one without symmetrical boundaries (Model 2) and the other with multiple blocks orientated perpendicular to the direction of wave propagation but with symmetrical boundaries (Model 3). Model 3 could be considered not to be a 1D model due to the stack of blocks perpendicular to the direction of wave propagation. These are solved in the DEM-FDM model due to limitations in the boundary conditions and intersecting of joints imposed by the FDM code of Hildyard et al. [29]. Finite joints are to all intents guaranteed in nature, as joints cannot be continuous, even if they are highly persistent. Therefore, testing this assumption means the model will be more realistic. The blocky rock mass in Model 3 contains finite joints, but also tests whether the resonance mechanism occurs when an additional joint set is modelled, orientated perpendicular to the first joint set. The FDM model is a two-dimensional (2D) plane strain model with an excitation located at a single node in its centre (Model 4), generating a non-planar wave. Non-planar waves are likely in nature, as many of the common vibrational sources given in Fig. 1 will originate as a point source. Waves will spread out radially from the point source, breaking the plane wave assumption. The FDM code is adopted because of limitations in

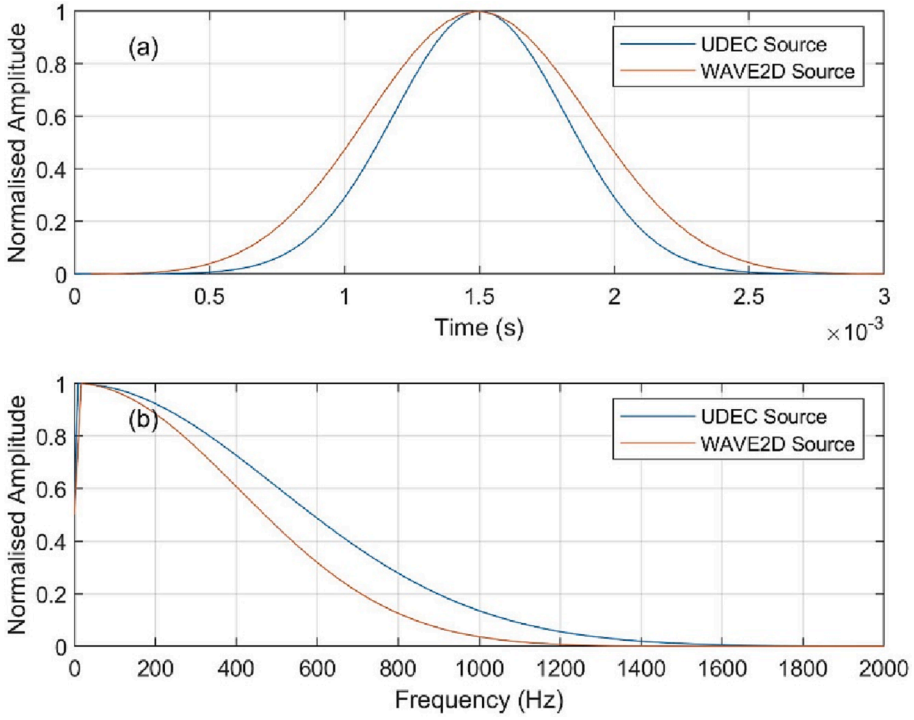

Fig. 2. Input waves to UDEC and WAVE2D models from [4]: (a) Time series of sources, and (b) Frequency content of sources. UDEC is a 500 Hz Gaussian wave and WAVE2D is a 500 Hz modified Ricker wave.

manually setting the time step of the models in the DEM-FDM model used for Models 2 and 3, which complicates the generation of the transfer functions.

Model 1 – 1D Model – DEM-FDM

A 1D model has been generated based on the model used by Holmes et al. [4], which is shown in Fig. 3. This is to provide a control to compare the results in the previous study. It was found that the single element thick model used in the previous study gives resonances which are lower than those predicted by Eqs. (5) to (7). In contrast, generating more than one element in the vertical direction gives resonances which more accurately match those predicted. This is likely to be due to boundary effects in the narrower model. A model height of 1 m is used, which is consistent with the model height used by Cai and Zhao [1], among others. A vertical mesh size of 0.25 m is generated, giving four elements in the direction perpendicular to wave propagation. The horizontal mesh size is 0.125 m. Given this mesh size and the properties given in Table 1, this model will be able to transmit frequencies up to 2662 Hz, based on the recommendations for the minimum wavelength to be at least ten times the mesh size [43].

Model 2 – No Symmetrical Boundaries – DEM-FDM

Model 2 is identical to the Model 1, shown in Fig. 3, without symmetrical horizontal boundaries. These boundaries are now modelled as being free. This model is solved using the DEM-FDM. Without symmetrical boundaries this model will not contain infinite joints, allowing the assumption of infinite joints to be tested. The model setup is shown in Fig. 4.

Model 3 – Blocky Material – DEM-FDM

Model 3 is a modified version of Model 1, with three blocks stacked on top of each other perpendicular to the direction of wave propagation. The vertical spacing of the joints is 1 m, so the model height has been increased to 3 m. The blocks represent finite joints, despite symmetrical boundaries being modelled. This gives an additional test of the infinite joint assumption, also tested in Model 2. The model set up is shown in Fig. 5. Horizontal and vertical joints have the same properties, as shown in Table 1. The mesh size remains as 0.25 m vertically and 0.125 m horizontally, as used in Models 1 and 2, also allowing frequencies up to 2662 Hz to be transmitted.

Model 4 – 2D Model – FDM

Model 4 is a 2D model with a source located in the centre of the model, which propagates outwards radially. The source applies a vertical point force to a single node in the centre of the model. The joints in this model are infinite; however, the wave is not a plane wave, allowing the plane wave assumption to be tested. The model set up is given in Fig. 6. A square finite difference mesh is generated within the model, with 0.1 m edge lengths. Frequencies up to 3328 Hz can be transmitted in Model 4, given that the mesh size is smaller than that used in Models 1 to 3. The difference in mesh size will not affect the transfer function below this maximum transmitted frequency. All external boundaries are modelled as absorbing.

Equivalent Material Models

Equivalent materials are investigated to determine whether the resonance effects are preserved when the method of representing joints is changed. The modelling is undertaken using a 1D FDM model using WAVE2D [29], shown in Fig. 7. This model is equivalent to Model 1, solved in a different software. This model has a mesh size of 0.08 m, with dimensions of 2080 × 4800 elements. With the material properties given in Table 1 this model will be able to transmit frequencies up to 4160 Hz. Again, this change in mesh size will not affect the transfer function below this maximum transmitted frequency.

Parastatidis [28] modelled jointed materials using three different material models: a discrete representation of joints (DM), a localised equivalent medium (LEM) and a homogenous equivalent medium (HEM). All three of these material models are used here, with the addition of a localised homogenous equivalent medium (LHEM). The LHEM only applies transversely isotropic material properties between the first and last joints. This will increase the *1/L* of that medium, and therefore change the material properties used in this area, when compared to the HEM. These material models are illustrated in Fig. 8. The LHEM is introduced as joints only fill a small portion of the model shown in Fig. 7, while they populate the entire model used by Parastatidis [28]. Due to the size of the model the effect of the joints in the HEM is diluted across the entire model, while the effect of the joints in the LHEM is contained between the first and last joint, which can be thought of as the jointed region of the model.

Transfer Functions

Transfer functions are used to analyse the data from the models used in this study. These are generated using Eq. (8). Data is recorded giving an input waveform (u_{ref}) and an output waveform (u), which are transformed into the frequency domain using a Fourier transform (to give u'_{ref} and u'). These show how elements introduced into a propagation pathway can affect the amplitude of vibrations as the frequency of the vibration changes. The results are interpreted as Transmission Coefficients (TC) and plotted against the frequency of the vibration. A TC equal to one shows that the vibration at that frequency is not affected by a model, while values greater than one show an increase in the vibration amplitude and less than one a reduction in the amplitude. As this method gives the relative difference between the amplitude of vibrations at different frequencies, it is possible to compare different models which have been excited by different waveforms. Therefore, the different excitations used in the models in this study, as described in the previous sections, will not affect the results, and the transfer functions derived can be applied to complex vibrational sources, such as rail vibrations.

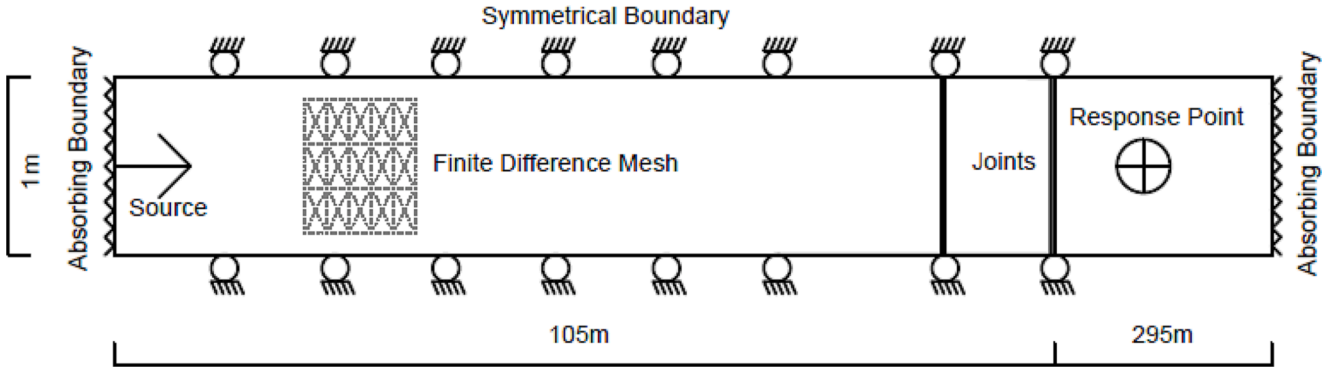

Fig. 3. DEM-FDM Model 1 (adapted from Holmes et al. [4]) showing finite difference mesh for finite joint verification case. Mesh fills entire model. Not to scale.

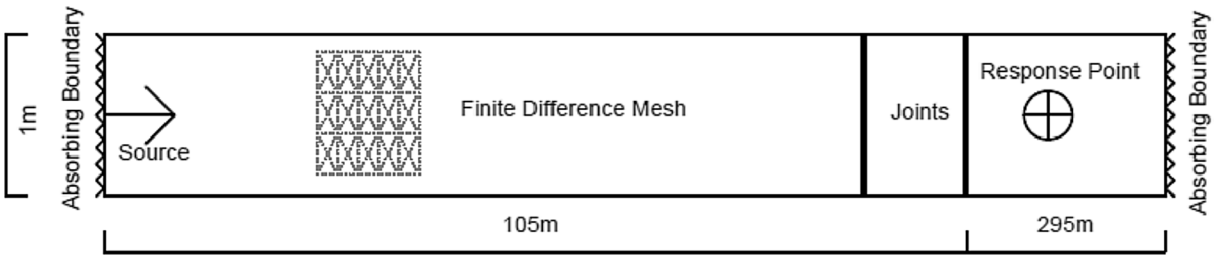

Fig. 4. DEM-FDM Model 2 with no symmetrical boundaries showing finite difference mesh for finite joint verification case. Mesh fills entire model. Not to scale.

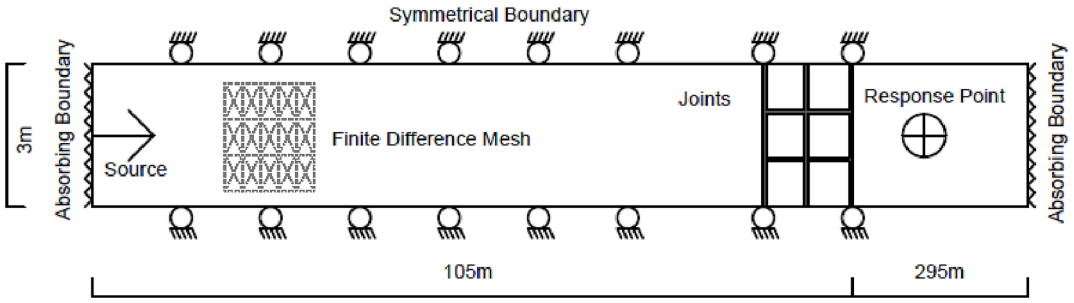

Fig. 5. DEM-FDM Model 3 with multiple blocks showing finite difference mesh for finite joint verification case. Mesh fills entire model. Not to scale.

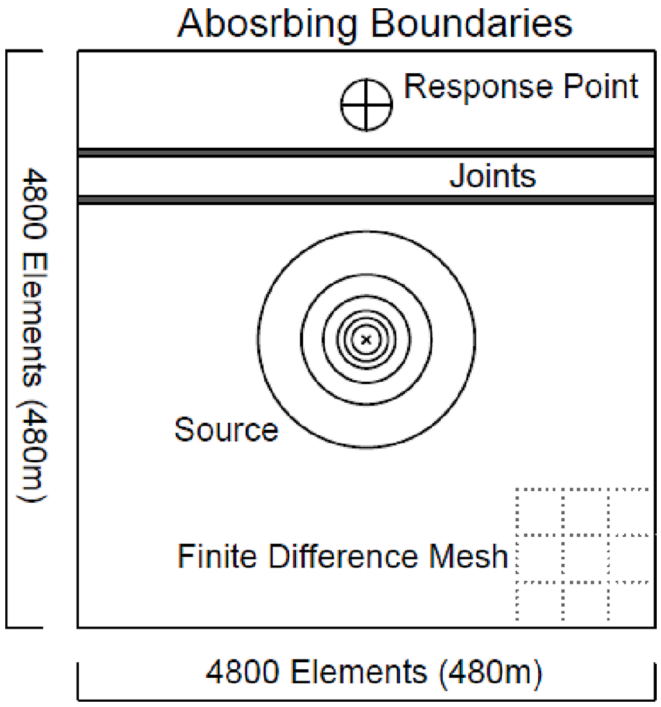

Fig. 6. 2D FDM Model 4 showing finite difference mesh for finite joint verification case. Mesh fills entire model. Not to scale.

$$TC = \frac{u'_{ref}}{u'} \tag{8}$$

The transfer functions from Models 1–3 and the equivalent material models are generated by using a velocity–time history close to the source for the input and the velocity–time history after the joints as the output. However, in Model 4, due to geometrical damping, inevitable during the propagation of a non-planar wave, this procedure cannot be used. If the effects of damping were included in the calculation of the transfer functions the effect of joints could be hidden. To overcome this the transfer function is generated as a reduction factor, which are often used when evaluating the performance of wave barriers [14]. This is undertaken by comparing the response of an identical model without joints with the jointed model, with measurements taken at identical locations in both models. The geometrical damping will be similar in both models, largely removing this effect from the calculation of the transfer function. Therefore, any differences in the waveforms will be caused by the presence of the joints within the model.

Results

Discrete Jointed Models

Fig. 9 shows the results from Models 1 to 4, along with the analytical results, from equations (5) and (6). This Figure shows that all the models display comparable results, with maxima at comparable frequencies to the resonance predicted by the analytical function (Eqs. (5) and (6), at 96 Hz. There are minor differences in the peak frequency in all the models, although all of these are broadly the same frequency.

Despite the similarities none of the models exactly match the results of the 1D, infinite jointed, Model 1. The 2D Model 4 shows a transmission coefficient of 0.92 at the resonant frequency, while the other models show a transmission coefficient of approximately 1 at this frequency. Equally, the transmission coefficient at 0 Hz is much lower in Model 4 than in the other models. The local minimum, at approximately 50 Hz, is also lower than the other models and the higher frequency transmission coefficients are also slightly different. The differences observed in the transmission coefficients of Model 4, relative to Model 1, are likely to be due in part to the different method of generating the transfer function for this model, but also refraction of the waves when they are incident upon the joints at non-normal angles. This is a consequence of the 2D nature of Model 4, so will not occur in the other models, and is likely to have affected the transfer function.

The finite jointed Model 2 and the blocky Model 3 have similar transfer functions to Model 1, with similar high frequency content as well as similar transmission coefficients at the resonant frequency and at 0 Hz. However, there are differences at the local minima in the transfer functions at approximately 50 Hz. Model 2 shows an undulating transfer function here, with a higher transmission coefficient than Model 1.

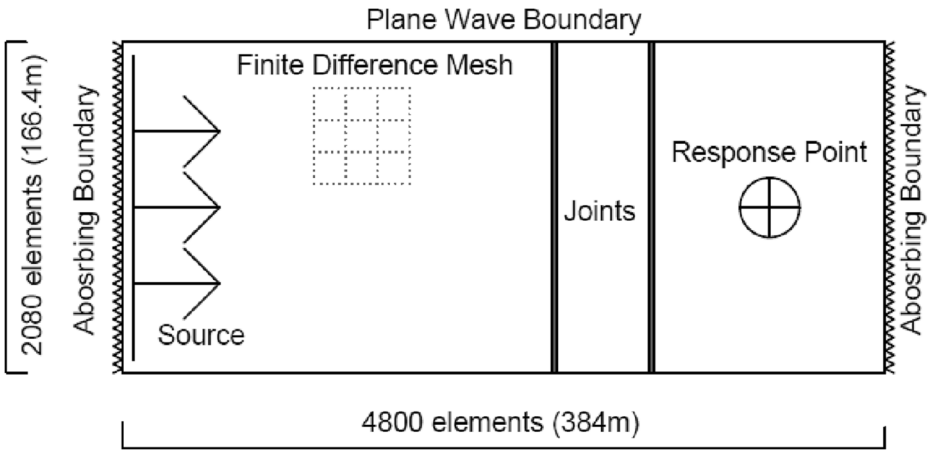

Fig. 7. FDM model showing finite difference mesh used with equivalent material models.

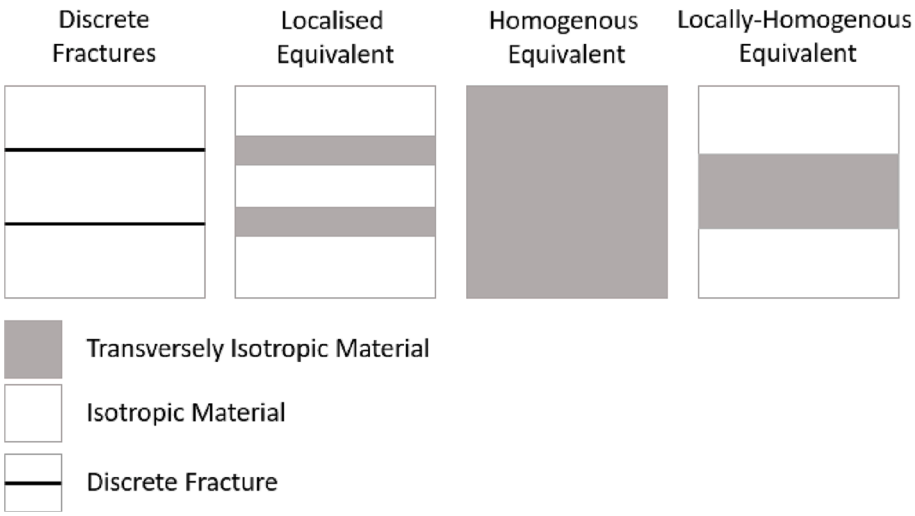

Fig. 8. Equivalent material models used in study.

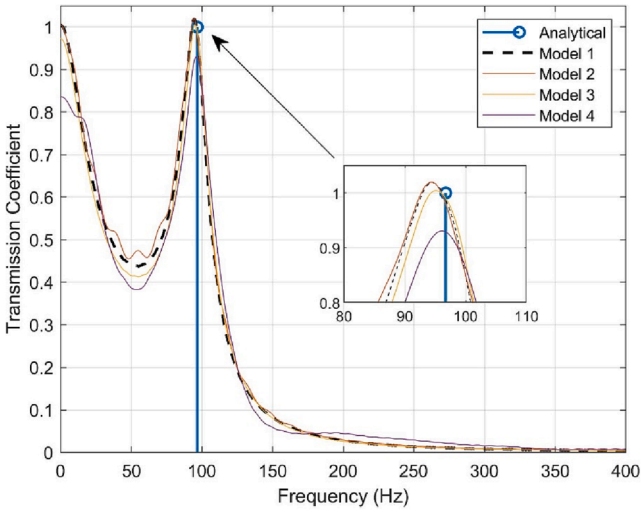

Fig. 9. Transfer functions for Models 1 to 4 and Analytical Function.

Model 3 shows a smooth transfer function, but at a lower transmission coefficient when compared to Model 1. The differences observed in the transmission coefficients of Models 2 and 3 are due to the different modelling assumptions used, as all other inputs and the signal processing are identical.

As Model 4 is 2D it is possible to view the transmission of waves across a surface within the model. This shows transmission of waves out of the propagation pathway directly above the source, as shown in previous figures. Fig. 10 shows the results from Model 4 as a 1D surface transfer function. This is generated by adding in extra, evenly spaced, response points along a surface in the model. The offset in Fig. 10 refers to the distance from the centre of model, directly above the source. Transfer functions are generated for each of these points, which are meshed and plotted as a contour plot. As the results for different offsets are generated using the same modelling run, the transfer function at 0 m offset is identical to that shown inFigure 9, for Model 4. Fig. 10 shows the analytical spring resonance predictions, from Eqs. (5) and (6), as a dashed black line. This Figure shows that these effects persist for offsets between +/- 20 m from the application of the load. There is some degree of frequency spreading of the high transmission zone at large offsets; however, it still occurs at the frequency predicted for spring resonance.

Equivalent Material Models

The model presented in Fig. 7 is modelled with the different equivalent materials shown in Fig. 8. The results for this are shown in Fig. 11. The DM results are similar to those for Model 4, although not identical as model 4 is a 2D model with a non-plane wave and the DM results are

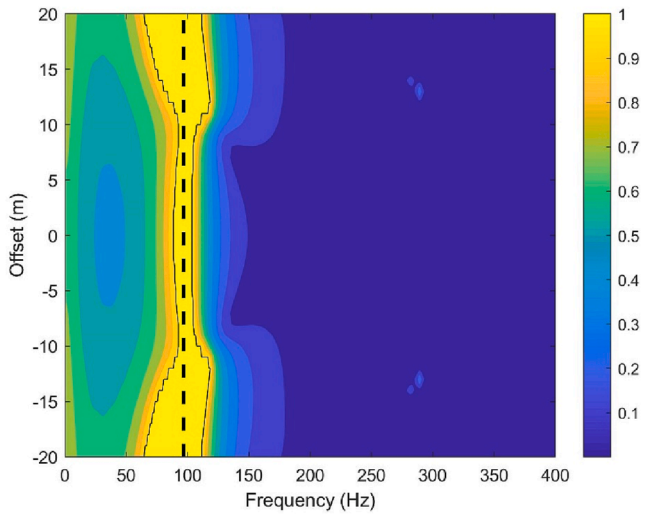

Fig. 10. 1D surface transfer functions from the FDM Model 4, infinite and finite jointed models and Analytical models. Colour bar indicates transmission coefficient. Black dashed line shows the predicted spring resonant frequency.

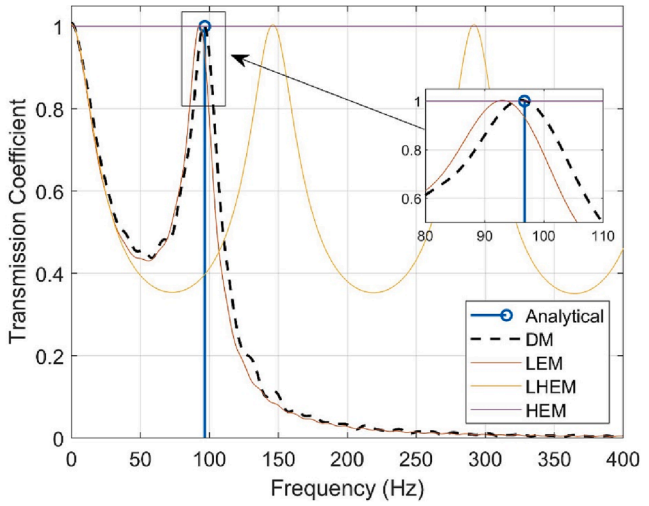

Fig. 11. Transfer functions for equivalent material models.

from an effectively 1D model with a plane wave. It is clear that there is an analogous profile to the transfer functions given by the DM and LEM models, with corresponding frequencies of local maxima. In the DM this occur at 96 Hz, while in the LEM this occurs at 92 Hz. These occur at similar frequencies to the analytical prediction of the spring resonance, occurring at 96 Hz, from Eqs. (5) and (6). The LHEM and HEM models show quite different transfer functions to the DM model. The HEM model shows a transmission coefficient equal to one at all frequencies. This is to be expected using a 1D model with no damping, as there is no potential for the wave to be modified during transmission. Up to 30 Hz the LHEM model shows similar transmission coefficients to the DM and LEM models. However, past 30 Hz the profiles of the transfer functions are quite different. The LHEM has an oscillation in the transfer function with maxima located at an even spacing of 146 Hz. This oscillating transfer function is likely to be related to the superposition of waves within the weaker, and therefore slower, block of equivalent material within the model. This is equivalent to the superposition resonance mechanism observed in jointed materials. This reduced stiffness block will not oscillate under the spring resonance mechanism as no joints, analogous to springs, are modelled.

Discussion

This study has tested various common modelling assumptions as well as material models to understand whether they influence the spring resonance mechanism identified in jointed rock masses and to assess whether such effects will occur in more complex, realistic scenarios. The assumptions tested in this study are symmetrical boundaries, infinite joints, and plane waves, as well as different methods of representing joints using different equivalent material models.

Regarding the modelling assumptions, despite some differences in the transfer functions shown in Fig. 9, this Figure shows evidence of a peak in the transfer function at the frequency expected for spring resonance in the models. The verification of the applicability of the spring resonance effect in this study suggests that these effects will persist in a wide range of rock masses and when plane wave conditions are not met.

There are minor differences in the transfer functions form Models 2 to 4, when compared to Model 1, although there are many similarities. For example, in Models 2 to 4 the amplitude of the transmission coefficients for resonant frequencies are clearly elevated, compared to surrounding frequencies. This implies that waves at the resonant frequency are not significantly attenuated as they pass through joints. This has important implications for stress wave propagation through jointed rock masses, as stress waves propagating at the resonant frequency of the rock mass will deliver higher amplitude vibrations to a receiver, relative to non-resonant frequencies. The resonant frequencies for a rock mass with a large number of joints will show a high transmission zone at low frequencies where the resonant peaks are squashed together between 0 Hz and a cut off maximum spring resonance for the given rock mass. For a rock mass with the properties given in Table 1 the cut off spring resonant frequency is 137 Hz. Therefore, the rock mass from Table 1 could have a high transmission zone up to 137 Hz, given a sufficiently large number of joints. Following the high transmission zone will be a low transmission zone. This means that the rock mass is acting as a low pass filter, only allowing the transmission of low frequency waves through the joints. This is illustrated using a FDM model with a large number of joints in Fig. 12. There are minima seen in the high transmission zone in the transfer function in Fig. 12; however, this is due to the small size of the model and therefore a limited number of joints compared to a realistic rock mass. Despite this, the resonant frequencies do merge close to the cut off frequency, giving a clear high transmission zone. Therefore, given a large number of joints, a jointed rock mass could have the same transmission coefficient as a continuum material at low frequencies. Schoenberg and Sayers [22] proposed a similar effect,

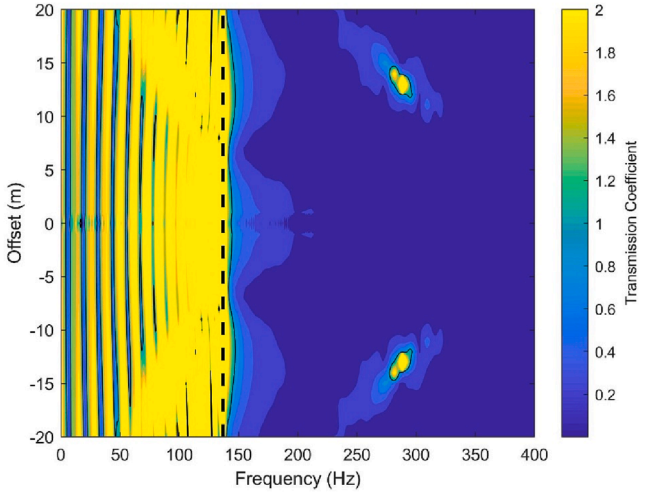

Fig. 12. Transfer function for a continuously jointed rock mass. Transmission coefficient is given by the colour bar and is relative to an unjointed continuum model. Black dashed line shows spring resonance (equations (5) and (6).

where when the wavelength is much larger than the joint spacing an equivalent continuum can be assumed. It is clear from the presence of the spring resonance mechanism that this equivalency can only be possible in rock masses with a large number of joints, or within a heterogeneous jointed material.

The maxima observed in Fig. 12 at frequencies of between 275 and 200 Hz and an offset of 15 m, are interpreted to be a superposition effect caused by refraction and superposition of shear and compressional waves caused by the joints within the 2D model. This is not the same superposition resonance predicted using Eq. (7), which is based on the reflection of normally incident waves upon joints, which will occur at 832 Hz.

The results from the equivalent material models are shown in Fig. 11. This shows that the DM and LEM show similar frequencies for the local maximum at 96 and 92 Hz, respectively. This matches the predicted spring resonance frequency for this rock mass. This shows that the spring resonance mechanism occurring in the DEM model also occurs in the LEM model, which has not previously been identified. Furthermore, the similarity in the frequency of the resonances show that the methodology for defining the equivalent medium properties using cracks per unit length (Eq. (4), gives an interface with a near identical stiffness to the discrete jointed model. With the slight difference generated through rounding errors associated with the calculation of 1/L. The HEM shows a transfer function equal to one at all frequencies, which would be expected for a 1D continuum model. The pattern in the transfer function for the LHEM shows successive peaks and troughs, separated by 146 Hz. This effect is generated due to the difference in stiffness of the equivalent material and the original isotropic material. This will allow stress waves to reflected from the interface between the different mediums and superimpose on each other, in a similar fashion to the superposition resonance mechanism. The spring resonance mechanism does not appear to develop. This is due to there being no joint present between the equivalent material and the original isotropic material, with the interface acting more akin to an infinite stiffness welded interface.

The experiments conducted in this study provide convincing evidence that the spring resonance does occur in simulations of jointed rock masses. However, as this study and the previous study of Holmes et al. [4] both use a numerical approach, physical evidence of the spring resonance mechanism is not provided. Examples can be found in studies relating to periodic metamaterials that show high transmission zones within frequency response functions, which are synonymous with the transfer functions presented in this study. Witarto et al. [35] presented a simple periodic metamaterial and analysed its performance using a frequency sweep on a shake table. Later, Huang et al. [14] modelled the same material using the finite-element method. The material being analysed was a concrete layer, sandwiched between polyurethane. Due to the stiffness difference in the materials, the polyurethane will act like a joint, while the concrete will act like a block. The properties of the materials used in the test are shown in Table 2, which give the spring resonance of this single block system as 8 Hz. Fig. 13 shows the frequency response function from the studies of Witarto et al. [35] and Huang et al. [14], along with the spring resonance frequency from Eqs. (5) and (6). This shows that the amplified frequencies found by the previous studies closely match the resonant frequency predicted by the analytical equations for spring resonance, giving convincing evidence

Table 2
Material properties of the periodic metamaterial [35].

Material	Property
Concrete	
Density	2300 kg/m^3
Elastic Stiffness	31400 MPa
Poisson's Ratio	0.2
Thickness	0.05 m
Polyurethane	
Stiffness	0.1586 MPa

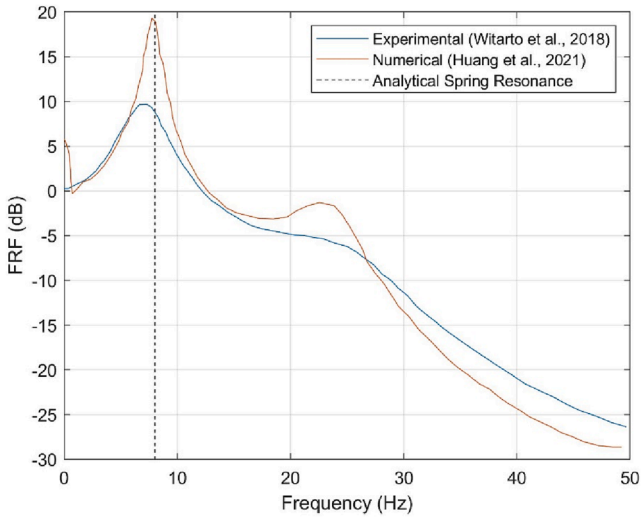

Fig. 13. Frequency response function for single block metamaterial from the laboratory experiment Witarto et al. [35] and corresponding numerical experiment of Huang et al. [14]. Analytical spring resonance from equations (5) and (6).

that the resonance effect can be isolated in physical models, and that it is a realistic phenomenon.

The amplification observed by Witarto et al. [35] and Huang et al. [14] in Fig. 13 is related to the unconfined block within the models, both physical and numerical, which are used in those studies. A stiff concrete layer was excited, with vibrations then propagating through the less stiff rubber layers. The rubber layers allow greater deformation, allowing the unrestrained end block to displace to a greater degree than the block which was excited. On the other hand, the models used in the current study have end blocks which are restrained. Therefore, despite the potential for the weaker layers representing the joints to increase the amplitude of vibrations, this does not occur in the figures presented in this study. The amplification of the end block does not change the resonant frequency of the mass-spring system, so the peak transmission still occurs at the same frequency as the spring resonant effect.

Following the similarities between the resonances identified by the analytical spring resonance equations and the physical experiment of Witarto et al. [35] it is reasonable to assume that such effects are also likely to occur in other physical systems, such as jointed rock masses. This is provided by the joints behaving elastically, like the polyurethane in the metamaterial. When applied to a realistic rock mass with a realistic vibration source, the implication of the presence of the spring resonance high transmission zone is that certain vibration sources can be transmitted, while others will not be. Fig. 14 shows the range of frequencies generated by common train and track vibrational sources from high speed rail. These are plotted against the maximum frequency of the spring resonance zone for common rock masses. The properties of the rock masses used for this are taken from Bandis et al. [42] and are included in Table 3, along with representative block material properties for each rock mass with maximum and minimum joint stiffnesses (fresh and weathered conditions, respectively) and joint spacings. The range of joint spacings were based on engineering judgement and in accordance with discontinuity descriptions in BS5930 [44]. These values are inputted to Eqs. (5) and (6) to give the maximum and minimum cut off frequencies for the spring resonance high transmission zone when there are a large number of joints within a rock mass.

Fig. 14 shows the maximum frequency of the spring resonance mechanism for a range of common rock types in different rock mass conditions. Eqs. (5) and (6) show that a higher maximum spring resonance frequency is given by a rock mass with small blocks and strong joints, while a low maximum frequency is given by large blocks with

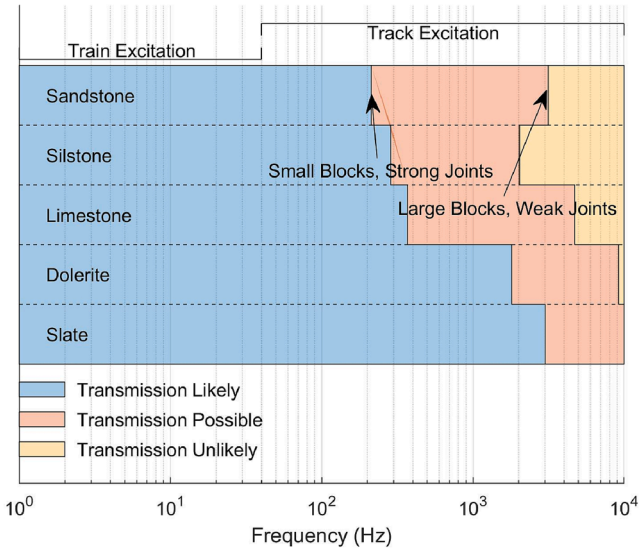

Fig. 14. Spring resonance high transmission zones for different rock masses plotted with ranges of train and track excitation frequencies from Connolly et al. [10]. They coloured boxes refer to the cut off frequencies of the spring resonance mechanism for different rock mass conditions, resulting in different probabilities of transmission through a rock mass.

weak joints. These conditions do not typify a strong or weak rock mass. A weak rock mass would be a combination of these two end members, with weak joints and small blocks. It is likely that for many rock masses encountered in the field the maximum spring resonance will fall between the two extreme cases. These end members have been used to designate the likelihood of vibrations being transmitted. All vibrations below the lower bound maximum frequency for the rock type are likely to be transmitted, and those above the upper bound maximum frequency unlikely to be transmitted. Between these frequencies it is possible that frequencies could be transmitted. Based on the zones in Fig. 14 all vibrations generated by the train are likely to be transmitted through a jointed rock mass, while some track excitations may not be.

When comparing the transmission of stress waves in a continuum and a discontinuum, the spring resonance mechanism will not occur in the continuum. This is because the movement of the blocks, which are not present in a continuum, generate the observed resonances. With no barriers to affect the transmission of stress waves, an undamped continuum model will have a transmission coefficient equal to 1 at all frequencies. Therefore, the entire transfer function can be thought of as a high transmission zone. While the high transmission zone is the most striking part of a jointed rock mass transfer function, it is in fact the low transmission zone outside of this which causes the transfer function of a discontinuum to vary from that of a continuum. Neglecting the effects of geometrical and material damping, within a continuum material all frequencies generated by a train will be transmitted with a transmission coefficient of one, as shown by the HEM model in Fig. 11. For a discontinuum material, such as the rock masses included in Fig. 14, only the frequencies which occur in the high transmission zone will be transmitted to a significant degree, with all frequencies which occur outside this zone being effectively eliminated. Consequently, high frequency vibrations are unlikely to be transmitted through a jointed rock mass. High frequency vibrations are produced more by high speed rail, relative to other forms of rail traffic, although they also generate low frequency vibrations. Therefore, high speed rail trains with transmission pathways through jointed rock masses will not transmit a considerable proportion of the vibration spectra unique to high speed rail. Despite this, high amplitude low frequency vibrations can still be transmitted through rock masses.

The models used in this study have attempted to see how modelling assumptions can affect the response of a model. However, with any numerical model, there are modelling assumptions still used in the generation of the models. Assumptions such as non-linear material properties, in-situ stresses and fully 3-dimensional (3D) settings have not been discussed. For example, Parastatidis [28] showed that an FDM model using a stress dependent joint constitutive model can more accurately match transmitted waveforms from experimental results. As such, there are many assumptions which have not been investigated in this study, although the models used here do support the theory that the observed resonance mechanisms will occur in physical jointed materials.

Conclusions

This study has shown that resonance effects, predicted by closed form analytical equations, occur in complex and realistic rock masses, including with finite and blocky joints, as well as with certain equivalent material models. The models analysed in this study represent more realistic scenarios which will be encountered in nature. Homogenous equivalent models of jointed rock masses do not exhibit resonance characteristics, while the discrete and localised equivalent materials do show the spring resonance effect. These resonance effects cause jointed materials to behave similar to periodic metamaterials. A bespoke analysis has been run to test modelling assumptions, with these compared to a 1D model and the analytical functions for spring resonance. Each model shows convincing maxima at the resonant frequency of the jointed rock mass to suggest that the resonance mechanism occurs. These validations show that the spring resonance effect is likely to occur in natural rock masses, including more complex blocky rock masses with additional joint sets. For rock masses with a large number of joints, a cut off frequency is introduced to indicate the maximum frequency of the spring resonance effect. This represents the maximum frequency of a high transmission zone, generated by spring resonance, meaning that the rock mass operates like a low pass filter up to this frequency.

Credible evidence is presented from published literature of the presence of the spring resonance effect in a physical model. This is found to occur in a periodic metamaterial, with the analytical equations for the spring resonance effect predicting the frequency accurately. The previous studies tested a periodic metamaterial in physical and numerical experiments, using an additional code which has not been used in this study. This shows that the spring resonance effect occurs in laboratory scale physical experiments, giving support to the hypothesis that this effect will occur in natural materials.

Jointed rock mass transfer functions are discussed in relation to rail vibration sources. This is undertaken using common rock masses with

Table 3
Properties used for resonance ranges in Fig. 14. All properties from Bandis et al. [42], except joint spacing which were based on engineering judgement in accordance with BS EN ISO 14689 Part 1 [44].

Rock Type	Block Elastic Stiffness (GPa)	Density (Mg/m^3)	Fresh Joint Stiffness (GPa/m)	Weathered Joint Stiffness (GPa/m)	Max. Joint Spacing (m)	Min. Joint Spacing (m)
Sandstone	24.0	2.41	34.9	8.8	6	0.06
Siltstone	28.5	2.42	64.2	20.0	6	0.2
Limestone	49.0	2.73	133.5	39.8	6	0.06
Dolerite	78.0	2.90	75.3	24.7	0.2	0.006
Slate	66.0	2.77	344.3	19.1	0.06	0.006

characteristic material properties and block sizes. It is concluded that the cut off frequency describes the upper limit of frequencies which will be transmitted through a jointed rock mass. This indicates that high speed rail sources located in a jointed rock mass, which are likely to generate high frequency vibrations, may be entirely cut out by the presence of the joints. In contrast, high amplitude low frequency vibrational sources, such as freight trains, are likely to be more problematic in jointed rock masses, than high frequency vibrations.

CRediT authorship contribution statement

Harry Holmes: Conceptualization, Methodology, Writing – original draft. **Chrysothemis Paraskevopoulou:** Supervision. **Mark Hildyard:** Supervision. **Krishna Neaupane:** Supervision. **David P. Connolly:** Supervision.

Declaration of Competing Interest

The authors declare the following financial interests/personal relationships which may be considered as potential competing interests: This work was supported by the Engineering and Physical Sciences Research Council (EPSRC) (funding award number EP/R513258/1).

Data availability

No data was used for the research described in the article.

Acknowledgements

This work was supported by the Engineering and Physical Sciences Research Council (EPSRC) (EP/R513258/1)

References

[1] Cai JG, Zhao J. Effects of multiple parallel fractures on apparent attenuation of stress waves in rock masses. Int J Rock Mech Min Sci 2000;37(4):661–82.
[2] Zhao J, Zhao XB, Cai JG. A further study of P-wave attenuation across parallel fractures with linear deformational behaviour. Int J Rock Mech Min Sci 2006;43(5):776–88.
[3] Pyrak-Nolte LJ, Myer LR, Cook NGW. Anisotropy in seismic velocities and amplitudes from multiple parallel fractures. J Geophys Res Solid Earth 1990;95:11345–58.
[4] Holmes H, Paraskevopoulou C, Hildyard M, Neaupane K, Connolly DP. Numerical Modelling of Resonance Mechanisms in Jointed Rocks using Transfer Functions. J Rock Mech Geotech Eng 2023;15(5):1076–89.
[5] Hussein MFM, Hunt HEM. A numerical model for calculating vibration due to a harmonic moving load on a floating-slab track with discontinuous slabs in an underground railway tunnel. J Sound Vib 2009;321(1-2):363–74.
[6] Ruiz JF, Soares PJ, Alves Costa P, Connolly DP. The effect of tunnel construction on future underground railway vibrations. Soil Dyn Earthq Eng 2019;125:105756.
[7] Eitzenberger A. Wave propagation in rock and the influence of discontinuities. Luleåtekniska universitet 2012.
[8] Sheng X. A review on modelling ground vibrations generated by underground trains. Int J Rail Transp 2019;7(4):241–61.
[9] Avci O, Bhargava A, Nikitas N, Inman DJ. Vibration annoyance assessment of train induced excitations from tunnels embedded in rock. Sci Total Environ 2020;711:134528.
[10] Connolly DP, Kouroussis G, Woodward PK, Giannopoulos A, Verlinden O, Forde MC. Scoping prediction of re-radiated ground-borne noise and vibration near high speed rail lines with variable soils. Soil Dyn Earthq Eng 2014;66:78–88.
[11] Hildyard MW. Manuel Rocha Medal Recipient Wave interaction with underground openings in fractured rock. Rock Mech Rock Eng 2007;40(6):531–61.
[12] Stolarik M, Pinka M, Nedoma J. Ground-borne vibration due to construction works with respect to brownfield areas. Appl Sci 2019;9:3766.
[13] Michel C, Guéguen P, El Arem S, Mazars J, Kotronis P. Full-scale dynamic response of an RC building under weak seismic motions using earthquake recordings, ambient vibrations and modelling. Earthq Eng & Struct Dyn 2010;39:419–41.
[14] Huang HW, Wang J, Zhao C, Mo YL. Two-dimensional finite-element simulation of periodic barriers. J Eng Mech 2021;147(2).
[15] Ouakka S, Verlinden O, Kouroussis G. Railway ground vibration and mitigation measures: benchmarking of best practices. Railw Eng Sci 2022;30(1):1–22.
[16] Connolly DP, Marecki GP, Kouroussis G, Thalassinakis I, Woodward PK. The growth of railway ground vibration problems — A review. Sci Total Environ 2016;568:1276–82. https://doi.org/10.1016/j.scitotenv.2015.09.101.
[17] Kuo KA, Hunt HEM, Hussein MFM. The effect of a twin tunnel on the propagation of ground-borne vibration from an underground railway. J Sound Vib 2011;330(25):6203–22.
[18] Forrest JA, Hunt HEM. Ground vibration generated by trains in underground tunnels. J Sound Vib 2006;294(4-5):706–36.
[19] Pyrak-Nolte LJ, Myer LR, Cook NGW. Transmission of seismic waves across single natural fractures. J Geophys Res Solid Earth 1990;95:8617–38.
[20] Fan Z, Zhang J, Xu H, Wang X. Transmission and application of a P-wave across joints based on a modified g-λ model. Int J Rock Mech Min Sci 2022;150:104991.
[21] Wang L, Wu C, Fan L, Wang M. Effective velocity of reflected wave in rock mass with different wave impedances of normal incidence of stress wave. Int J Numer Anal Methods Geomech 2022;46(9):1607–19.
[22] Schoenberg M, Sayers CM. Seismic anisotropy of fractured rock. Geophysics 1995;60(1):204–11.
[23] Deng XF, Zhu JB, Chen SG, Zhao J. Some fundamental issues and verification of 3DEC in modeling wave propagation in jointed rock masses. Rock Mech Rock Eng 2012;45(5):943–51.
[24] Zhu JB, Zhao XB, Li JC, Zhao GF, Zhao J. Normally incident wave propagation across a joint set with the virtual wave source method. J Appl Geophys 2011;73(3):283–8.
[25] Zhu JB, Deng XF, Zhao XB, Zhao J. A numerical study on wave transmission across multiple intersecting joint sets in rock masses with UDEC. Rock Mech Rock Eng 2013;46(6):1429–42.
[26] Fan LF, Wang LJ, Wu ZJ. Wave transmission across linearly jointed complex rock masses. Int J Rock Mech Min Sci 2018;112:193–200.
[27] Xu C, Liu Q, Wu J, Deng P, Liu P, Zhang H. Numerical study on P-wave propagation across the jointed rock masses by the combined finite-discrete element method. Comput Geotech 2022;142:104554.
[28] Parastatidis E. How do seismic waves respond to fractures in rock? Evaluation of effective media versus discrete fracture representations. University of Leeds; 2019.
[29] Hildyard MW, Daehnke A, Cundall PA, et al. A computer program for investigating elastodynamic issues in mining. 35th US Symp rock Mech 1995.
[30] Coates RT, Schoenberg M. Finite-difference modeling of faults and fractures. Geophysics 1995;60(5):1514–26.
[31] Nakagawa S. Acoustic resonance characteristics of rock and concrete containing fractures. Berkeley: University of California; 1998.
[32] Li S, Tian S, Li W, Yan T, Bi F. Research on the resonance characteristics of rock under harmonic excitation. Shock Vib 2019;2019:1–11.
[33] EN BS. 14146: 2004 Natural stone test methods–Determination of the dynamic modulus of elasticity (by measuring the fundamental resonance frequency). Brussels, CEN 2004.
[34] Cummer SA, Christensen J, Alù A. Controlling sound with acoustic metamaterials. Nat Rev Mater 2016;1:1–13.
[35] Witarto W, Wang SJ, Yang CY, Nie X, Mo YL, Chang KC, et al. Seismic isolation of small modular reactors using metamaterials. AIP Adv 2018;8(4):045307.
[36] Hussein MI, Leamy MJ, Ruzzene M. Dynamics of phononic materials and structures: Historical origins, recent progress, and future outlook. Appl Mech Rev 2014;66.
[37] Castanheira-Pinto A, Alves-Costa P, Godinho L, Amado-Mendes P. On the application of continuous buried periodic inclusions on the filtering of traffic vibrations: A numerical study. Soil Dyn Earthq Eng 2018;113:391–405.
[38] Zhao XB, Zhao J, Cai JG, Hefny AM. UDEC modelling on wave propagation across fractured rock masses. Comput Geotech 2008;35(1):97–104.
[39] Hildyard MW. Wave interaction with underground openings in fractured rock. Citeseer 2001.
[40] Itasca Consulting Group Inc. UDEC - Universal Distinct Element Code Version 6.0 2014.
[41] Connolly DP, Kouroussis G, Woodward PK, Costa PA, Verlinden O, Forde MC. Field testing and analysis of high speed rail vibrations. Soil Dyn Earthq Eng 2014;67:102–18.
[42] Bandis SC, Lumsden AC, Barton NR. Fundamentals of rock joint deformation. Int J Rock Mech Min Sci Geomech Abstr 1983;20(6):249–68.
[43] Kuhlemeyer RL, Lysmer J. Finite element method accuracy for wave propagation problems. J Soil Mech Found Div 1973;99(5):421–7.
[44] BSI. Code of practice for ground investigations BS 5930:2015+A1:2020. British Standards Institution London; 2020.